EMERGENCE OF DARK ZNO NANORODS BY HYDROGEN PLASMA TREATMENT

[1]Zdenek REMES, [1]Maksym BURYI, [1]Dhananjay K. SHARMA, [1]Anna ARTEMENKO,
[2]Julia MICOVA, [3]Bohuslav REZEK, [4]Ales PORUBA, [5]Hua Shu HSU, [1]Stepan Potocky,
[1]Vladimir BABIN

[1]Institute of Physics, Czech Academy of Sciences, Prague, Czech Republic, EU,
remes@fzu.cz, buryi@fzu.cz, dhananjay@fzu.cz, artemenko@fzu.cz, potocky@fzu.cz, babin@fzu.cz

[2]Institute of Chemistry, Slovak Academy of Sciences, Bratislava, Slovakia, EU, chemjumi@savba.sk

[3]Faculty of Electrical Engineering, Czech Technical University, Prague, Czech Republic, EU,
rezekboh@fel.cvut.cz

[4]SVCS Process Innovation s.r.o., Valasské Mezirici, Czech Republic, EU, aporuba@svcs.cz

[5]Department of Applied Physics, National Pingtung University, Taiwan, hshsu@mail.nptu.edu.tw

https://doi.org/10.37904/nanocon.2021.4374

Abstract

Plasma hydrogenation of hydrothermally grown ZnO nanorods was done at 13.56 MHz in inductively coupled plasma (ICP) with H_2/Ar gas mixture. Plasma was monitored by optical emission spectroscopy (OES) and by measuring self-bias potential of the stainless-steel sample holder isolated from the ground by a capacitor. The ZnO surface chemical composition was studied by XPS. The exciton-related UV photoluminescence of ZnO nanorods and optical absorption increased significantly after plasma treatment and diminished after plasma oxidation. Increasing Ar in hydrogen plasma caused more negative self-bias, less efficient hydrogenation and lower exciton photoluminescence. We attribute changes of optical properties to changes of surface and related electronic states giving also rise to its black color visually.

Keywords: Optical materials, ZnO, ICP, plasma hydrogenation, OES, XPS, photoluminescence

1. INTRODUCTION

The hydrothermally grown zinc oxide (ZnO) crystalline powder is a low cost and environmentally friendly material with unique optical properties and variety of nano and micro-structures. ZnO nanorods (ZnO NRs) with their high surface-to-volume ratio and related size effects impose challenges for energy conversion, scintillators, photocatalytic wastewater treatment, electrochemical energy storage or sensing applications [1]. For instance, black ZnO nanoparticles prepared by heating in hydrogen atmosphere at 400 °C for 2h displayed long-wavelength absorption and improved photocatalytic performance [2].

We have built inductively coupled plasma (ICP) reactor with up to 300 W discharge power operating at the radio frequency 13.56 MHz for plasma hydrogenation of powder samples. Plasma contains energetic electrons, ions, excited radicals and molecules providing further adjustment of surface properties while keeping a sample at a relatively low temperature [3]. Plasma hydrogenation of ZnO NRs leads to a significant increase of exciton-related UV luminescence [4]. Their surface properties were examined by X-ray photoelectron spectroscopy. To further study such effects, we elucidate in this paper the key role of self-bias on the optical properties of ZnO NRs exposed to plasma in an ICP reactor with an ungrounded stainless-steel sample holder isolated from the ground by a blocking capacitor.

2. EXPERIMENTAL

2.1. Hydrothermal growth of ZnO nanorods

The synthesis of ZnO NRs was based on the reaction of an equimolar mixture of 25 mM analytical grade zinc nitrate hexahydrate $Zn(NO_3)_2{\cdot}6H_2O$ (250 mL) and hexamethylenetetramine $C_6H_{12}N_4$ (HMTA, 250 mL) without further purification. Both solutions were filtered through a Whatman 2 filter and mixed with vigorous stirring (700 rpm, 15 min). The hydrothermal growth was performed at 90 °C for 3 h. After cooling to room temperature, ZnO NRs were freed of residual salts by washing 5 times with distilled water, separated by centrifugation and lyophilized for 24 h. Finally, ZnO NRs were annealed in air at 350 °C for 15 min to prepare anhydride powder with improved crystal quality.

2.2. Inductively coupled plasma (ICP)

An inductively coupled plasma (ICP) reactor with quartz walls, developed in collaboration with the Czech company SVCS Process Innovation s. r. o. operates at the radio frequency (RF) 13.56 MHz with up to 300 W discharge power. It employs H_2, O_2, N_2, NH_3 and Ar process gasses with a flow rate up to 50 sccm. To repeal plasma from the reactor walls, the capacitive coupled plasma (CCP) mode was reduced by an electrically grounded electrostatic shield installed outside the reactor between the quartz walls and the RF coil. Plasma treatment of ZnO NR was performed using a stainless steel holder similar to an rotating cradle isolated from the ground by a blocking capacitor with an RF impedance of 50 Ω. Prior to plasma treatment, the chamber was evacuated for 30 min to a base pressure of less than 0.1 Pa and purged for 10 minutes with 50 sccm of process gas flow. The plasma hydrogenation was done for 30 min with RF power 100 W, 10 sccm H_2 and up to 2 sccm Ar gas flow. The plasma oxidation was done for 5 min with RF power 100 W and 10 sccm O_2. The self-bias potential of the holder was measured using an electrometer Keithley 6517A in a guarded DC mode.

2.3. Characterization

Optical emission spectra (OES) were measured in 400-900 nm spectral range with 1 nm spectral resolution by spectrally calibrated fiber coupled CCD spectrometer (B&W Tek BTC112E) optically focused in the middle of the quartz chamber just above the sample holder. The exposition time varied from 0.3 to 3 s depending on plasma luminosity. Each spectrum was averaged 10 times and the spectra were divided by the exposition time. Spectra obtained in dark were subtracted.

The X-ray photoelectron spectra were acquired at AXIS Supra photoelectron spectrometer (Kratos Analytical Ltd., UK) equipped with a monochromated Al Kα X-ray source (1486.6 eV) and hemispherical energy analyzer. ZnO NRs were pressed in pellets and fixed by Cu tape on the sample holder. The XPS survey spectra were collected at a pass energy of 80 eV whereas the high resolution (HR) spectra were acquired at the pass energy of 20 eV. XPS spectra were obtained at a constant take-off angle of 90˚ from the analysis area of 0.3×0.7 mm^2. The XPS spectra were measured with a charge neutralization system. Peak fitting of the measured high resolution spectra was performed by the CasaXPS software using Shirley background and Gaussian/Lorentzian line shapes (GL(30), 70% Gaussian and 30% Lorentzian) without fixing of peak width (full width at half maximum, FWHM). Binding energies of photoelectron lines were determined with an accuracy of ± 0.2 eV and referenced to C-C bonds in C 1s component at 285.0 eV [5].

Photoluminescence emission spectra (PL) were excited by pulsed, narrow band-pass UV LED (340 nm, 100 mW/cm^2, 333 Hz) and measured at room temperature in the 350–780 nm spectral range using a perpendicular geometry, long pass optical filters (LP350 and LP400 nm), a spectrally calibrated double gratings monochromator SPEX1672, a cooled multi-alkali photomultiplier tube, current preamplifier with a gain 10 μA/V and a dual-phase lock-in amplifier referenced to the UV LED frequency.

3. RESULTS AND DISCUSSION

Figure 1 compares OES of hydrogen plasma (10 sccm H_2) upon addition of Ar (0, 0.5, 1 and 2 sccm Ar). The OES spectra clearly show the presence of atomic hydrogen (H peaks at 656 and 486 nm) and several Ar peaks in near IR (750-850 nm) with increasing intensity correlating with Ar flow [6]. OES shows that Ar reduces luminosity of H peaks due to a plasma shield around the sample holder, see also **Table 1**. This is because the asymmetry of charging and discharging processes in RF plasma induces on ungrounded holder a negative steady-state self-biased floating potential that repels electrons from the holder and equalizes the electron and ion flows [7].

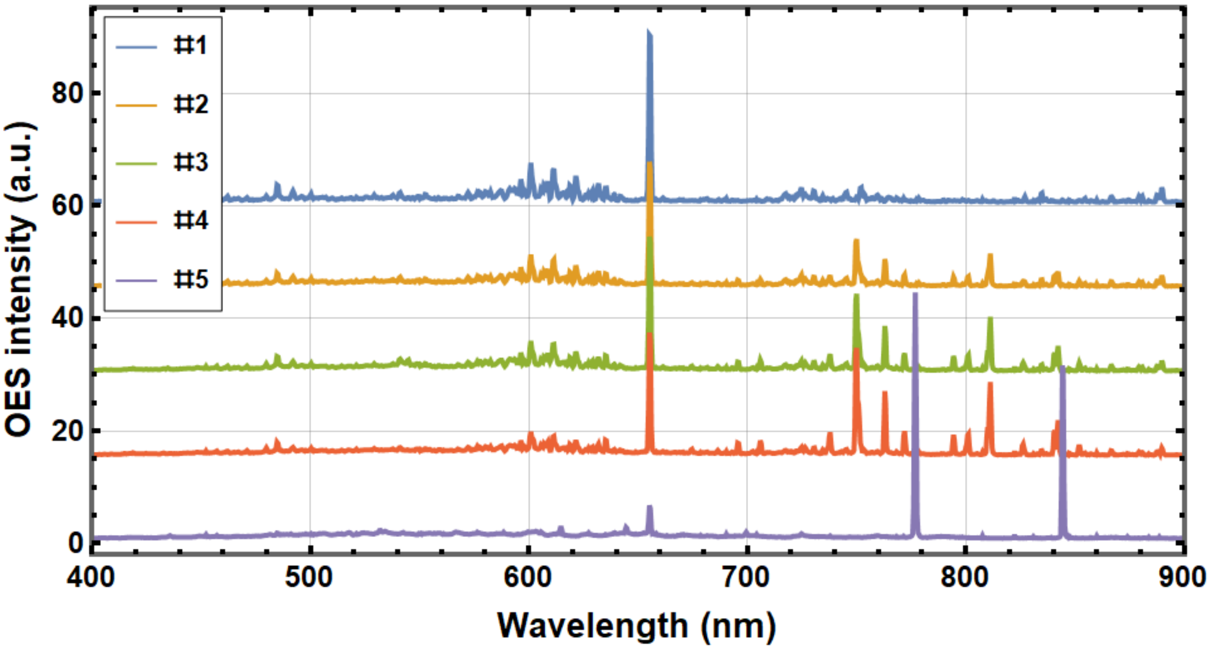

Figure 1 OES of hydrogen plasma upon addition of Ar (#1, #2, #3 and #4) compared to oxygen plasma OES (#5) measured with inserted hydrogenated ZnO sample.

Table 1 Gas flow, pressure, self-bias potential, integral intensity of H related OES at 653-659 nm, integral intensity of exciton-related UV PL (360-420 nm) and defect-related visible PL (480-780 nm). *Sample #5 was hydrogenated as #1 prior oxygen plasma treatment.

sample	H_2 flow (sccm)	Ar flow (sccm)	O_2 flow (sccm)	Gas pressure (Pa)	Self-bias (V)	OES @ 656 nm (a.u.)	UV PL (a.u.)	vis PL (a.u.)
#0	-	-	-	-	-	-	2 363	11 464
#1	10	0	0	6	-23.5	935	44 052	7 749
#2	10	0.5	0	11	-25.5	701	31 565	7 653
#3	10	1	0	9	-26.4	762	21 623	6 743
#4	10	2	0	11	-29.8	688	23 232	8 752
#5	0(10)*	0	10	9	-9.8	325	356	65 564

Two OES peaks at 635 & 637 nm are related to Si etched by hydrogen from quartz walls of the chamber. Oxygen plasma is dominated by strong IR peaks at 777 and 845 nm, but OES also shows that oxygen plasma releases some hydrogen from the previously hydrogenated ZnO NRs as demonstrated by the presence of the 656 nm peak (see #5 in **Figure 1**). No O peaks were detected in pure hydrogen plasma but small amount of O appears in H_2 & Ar plasma probably due to scattering of ZnO by heavy Ar ions.

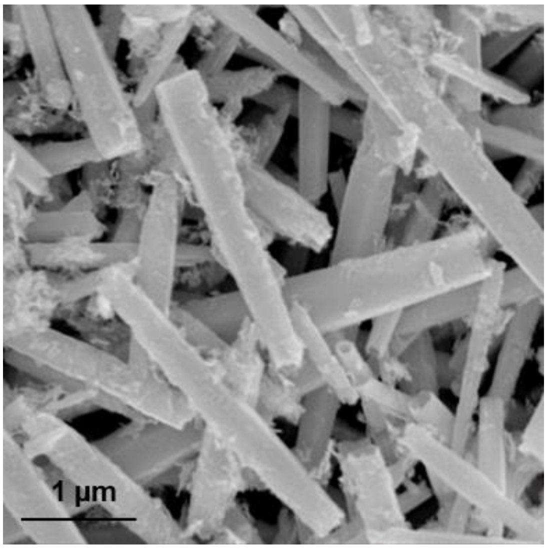

Figure 2 SEM image of hydrothermally grown ZnO NRs prior plasma treatment (MAIA3, TESCAN, 10 kV).

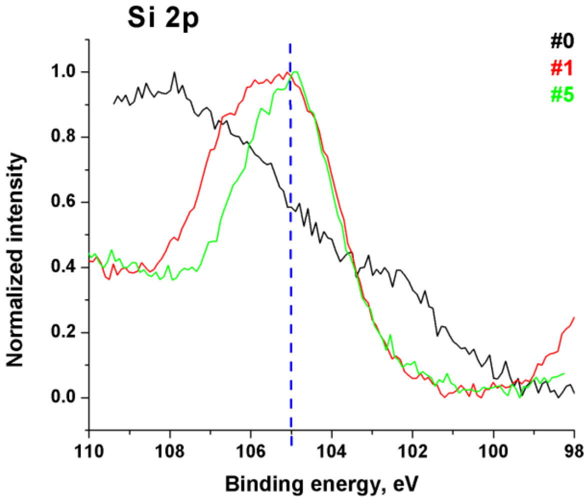

Figure 3 The comparison of normalized Si 2p XPS peaks of reference (#0), hydrogenated (#1) and oxidized (#5) ZnO.

Scanning electron microscopy (SEM) image of the synthetized ZnO NRs revealed crystallites with the hexagonal shape, the length about 2 µm and the diameter about 0.2 µm, see **Figure 2**.

Table 2 The atomic concentration of chemical elements calculated from HR XPS spectra of the plasma untreated sample (#0) and plasma hydrogenated sample (#1) subsequently plasma oxidized (#5).

sample	**Atomic concentration of chemical elements, at.%**						
	O	**C**	**Zn**	**Si**	**F**	**Cl**	**Ca**
#0	45.2	15.2	38.2	-	-	1.4	-
#1	52.0	11.6	19.3	11.0	2.9	2.0	1.2
#5	50.6	22.6	17.1	8.7	-	0.5	0.5

For the purpose of XPS studies, the reference sample (#0) was compared with the hydrogenated sample (#1) that was subsequently exposed for 5 min to oxygen plasma (#5). The Si 2p peak at about 104.9 eV were detected for plasma treated samples, see **Figure 3**. According to the Ref. [8], the Si signal can be attributed to SiF_4/Si. However, no F signal was observed in O_2 plasma treated ZnO NRs. **Table 2** shows that plasma hydrogenation caused increase of O content up to 52.0 at.% on the ZnO surface in contrast to reference sample (45.2 at.%) and the decrease of Zn to ~19 or even 17.1 at.% (after plasma oxidation) in comparison with initial values (38.2 at.%). On the other hand, hydrogen plasma treatment led to contamination of the ZnO surface with Si and Ca that comes probably from the quartz walls of the reactor chamber. The F signal (2.9 at.%) was detected after hydrogen plasma treatment (probably from the vacuum seals). Contamination by Si, Ca and F was reduced by plasma oxidation, thus it must be indeed surface related. Moreover, XPS analysis revealed that all ZnO samples were contaminated with C and Cl (probably a contamination from air or residual reactants used in hydrothermal growth of ZnO NRs).

The originally white reference sample became darker after plasma hydrogenation and white again after plasma oxidation as visualized by macro photographs, see **Figure 4**. Despite dark color, the PL spectrum of plasma hydrogenated ZnO NRs shows a strong exciton-related UV PL with the maximum at 380 nm and a low intensity of deep defect-related broad band in the red spectral region [9], see **Figure 5**. Plasma oxidation of the previously hydrogenated sample suppresses the exciton-related PL and strongly enhances the defect related

PL. This is a strong evidence that the observed optical properties after plasma treatment are caused by a complex changes of surface electronic states [10].

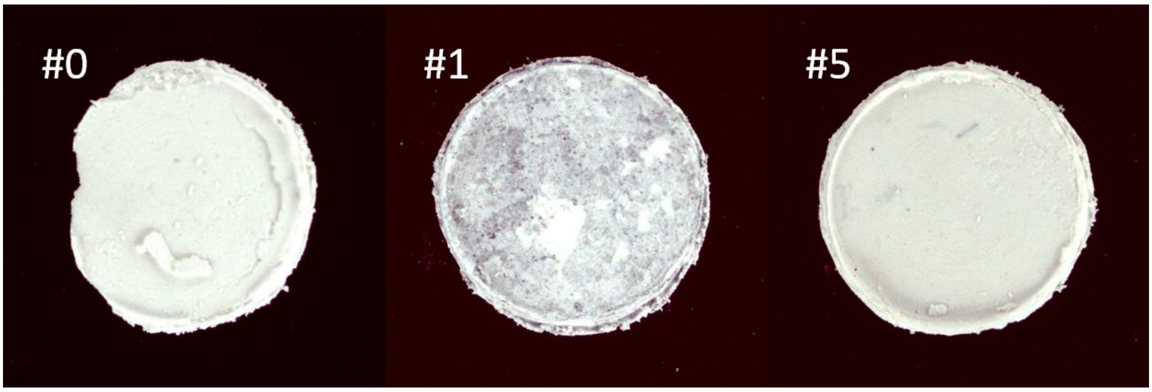

Figure 4 Macro photographs of plasma untreated (#0), plasma hydrogenated (#1) and plasma oxidized (#5) ZnO pellets (Ø 3 mm, 4 mg) taken with a macro objective (Lumix G Macro 30 mm, F2.8 ASPH)

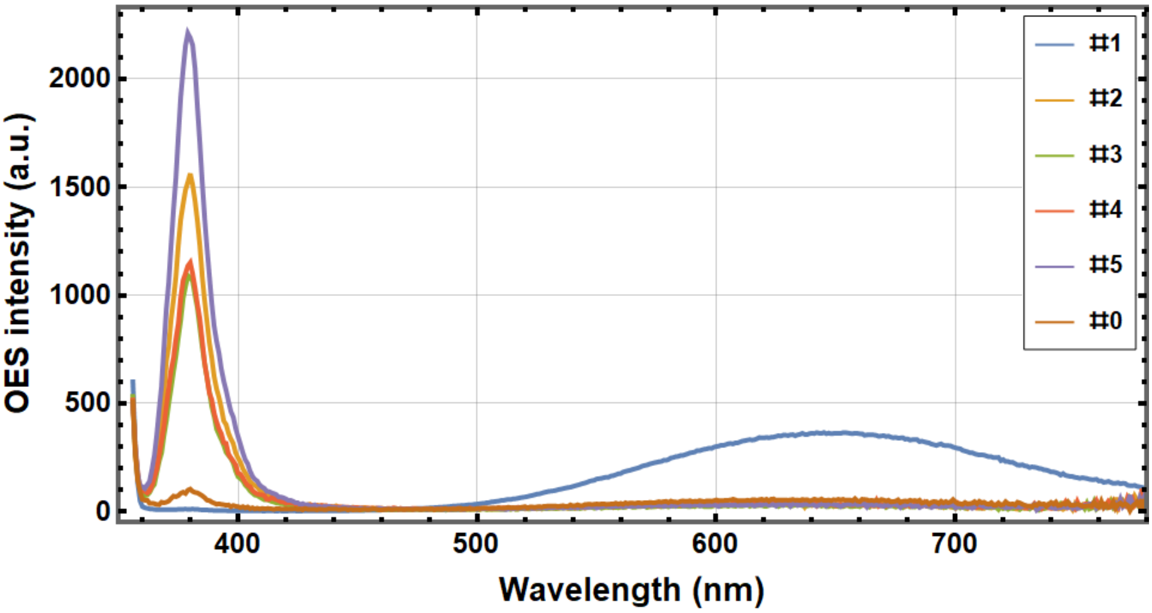

Figure 5 PL spectra of plasma hydrogenated ZnO upon addition of Ar (#1, #2, #3 and #4) compared to plasma oxidized (#5) and plasma untreated (#0) sample

4. CONCLUSION

Hydrothermally grown ZnO NRs were exposed to a hydrogen-argon plasma using a stainless-steel sample holder electrically isolated from the ground by a blocking capacitor. The PL spectra of plasma hydrogenated ZnO NRs show a strong exciton-related UV PL with a maximum at 380 nm, reduced red PL of defect states and increased absorption giving rise to its dark color visually. Changes in optical properties were attributed to complex changes in surface electronic states of ZnO NRs. Addition of Ar into hydrogen plasma caused more negative self-bias around the sample holder and less efficient plasma hydrogenation of ZnO NRs. Plasma oxygen treatment applied on hydrogenated ZnO NRs resulted in significantly reduced exciton-related UV PL and enhanced red PL associated with defects as well as reduced surface contamination by Si, Ca and F from quartz walls and vacuum seals of the ICP reactor. Further optimization of gas pressure, holder capacitance, and in-situ oxygen plasma treatment is required to obtain an optimally hydrogenated ZnO NRs with minimal contamination.

ACKNOWLEDGEMENTS

This work was supported by the Czech Science Foundation (GACR) project No. 19-02858J, CAS Mobility Plus project SAV-AVCR-21-09, Operational Program for Research, Development and Education project CZ.02.1.01/0.0/0.0/16_019/0000760 (Solid21), the Slovak Scientific Grant Agency (VEGA) grant 2/0157/20, the Ministry of Science and Technology of Taiwan (MOST) under the grant No. 108-2923-M-153-002-MY3, by the CzechNanoLab Research Infrastructure (MEYS CR, project no. LM2018110) and by the project Strategy AV21 (program Diagnostic Methods and Techniques). We thank R. Jackivová, J. Macíček and Yu Ying Chang for technical help.

REFERENCES

[1] KLINGSHIRN, C. F., ed. *Zinc Oxide: from fundamental properties towards novel applications*. Springer series in materials science. Heidelberg ; London: Springer, 2010, vol. 120. ISBN 978-3-642-10576-0.

[2] XIA, T., WALLENMEYER, P., ANDERSON, A., MUROWCHICK, J., LIU, L., CHEN, X. Hydrogenated black ZnO nanoparticles with enhanced photocatalytic performance. *RSC Adv*. 2014, vol. 4, pp. 41654–41658

[3] GRILL, A. *Cold plasma in material fabrication: from fundamentals to applications*. New York: The Institute of Electrical and Electronics Engineers, Inc., 1994.

[4] REMEŠ, Z., AUBRECHTOVÁ DRAGOUNOVÁ, K., MIČOVÁ, J. Plasma hydrogenation of hydrothermally grown ZnO micropods. In: *NANOCON 2020, 12th International Conference on Nanomaterials - Research & Application*: *NANOCON 2020- Conference Proceedings*. 2020, pp. 512–517

[5] MIČOVÁ, J., BURYI, M., ŠIMEK, D., DRAHOKOUPIL, J., NEYKOVA, N., CHANG, Y. Y., REMEŠ, Z., POP-GEORGIEVSKI, O., Jan SVOBODA, J., IM, Ch. Synthesis of zinc oxide nanostructures and comparison of their crystal quality. *Applied Surface Science*. 2018, vol. 461, pp. 190–195

[6] KRAMIDA, Alexander a Yuri RALCHENKO. *NIST Atomic Spectra Database, NIST Standard Reference Database 78*. National Institute of Standards and Technology. [online]. 1999. Available from: https://doi.org/10.18434/T4W30F

[7] BUTLER, H. S., KINO, G. S. Plasma Sheath Formation by Radio-Frequency Fields. *Physics of Fluids*. 1963, vol. 6, p. 1346.

[8] POWELL, C. *X-ray Photoelectron Spectroscopy Database XPS, Version 4.1, NIST Standard Reference Database 20*. National Institute of Standards and Technology. [online]. 1989. Available from: https://doi.org/10.18434/T4T88K

[9] BURYI, M., REMEŠ, Z., BABIN, V., NOVOTNÝ, M., VANĚČEK, V., AUBRECHTOVÁ DRAGOUNOVÁ, K., MIČOVÁ, J., LANDOVÁ, L., KUČERKOVÁ, R., MORE-CHEVALIER, J., CHERTOPALOV, S., FITL, P., KMJEČ, T. Influence of Mo doping on the luminescence properties and defect states in ZnO nanorods. Comparison with ZnO:Mo thin films. *Appl. Surf. Sci.* 2021, p. 149679.

[10] CHEN, X., LIU, L., LIU, Z., MARCUS, M. A., WANG, W.-Ch., OYLER, N. A., GRASS, M. E., MAO, B., GLANS, P. A., YU, P. Y., GUO, J., MAO, S. S. Properties of Disorder-Engineered Black Titanium Dioxide Nanoparticles through Hydrogenation. *Scientific Reports*. 2013, vol. 3, pp.1-7